DØ Note 5919-CONF

Version: 2.0

Measurement of the Dijet Mass Cross Section in $p\overline{p}$ Collisions at $\sqrt{s} = 1.96$ TeV

The DØ Collaboration
URL: *http://www-d0.fnal.gov*
(Dated: April 29, 2009)

The dijet mass spectrum is measured in $p\overline{p}$ collisions at $\sqrt{s} = 1.96$ TeV using 0.7 fb^{-1} of data collected with the D0 detector at the Fermilab Tevatron . The measurment is peformed in rapidity (y) regions up to $|2.4|$ for the two jets with the largest transverse momentum. NLO QCD calculations are found to be in reasonable agreement with the measured cross section.

I. INTRODUCTION

The dominant contribution to the total inelastic cross section in $p\overline{p}$ collisions at $\sqrt{s} = 1.96$ TeV is the production of jets from parton-parton interactions. Measurements of jet properties, such as the dijet mass spectrum, can be used to test the predictions of quantum chromodynamics (QCD), to constrain parton distribution functions (PDFs) within the proton, and to look for signatures of physics not predicted by the Standard Model. The measurement of the dijet mass spectrum is particularly sensitive to quark compositeness, extra spatial dimensions, and to unknown heavy particles that decay into two quarks [1]. Previous measurements of the dijet mass spectrum restricted the rapidity of the jets, $|y| < 1.1$ [2] where $y = 0.5 \ln[(E + p_L)/(E - p_L)]$ where E is the energy of the jet and p_L is the momentum along the direction of the proton beam. In this note, we measure the differential dijet mass spectrum up to $|y| < 2.4$. Measurements at high transverse momentum (p_T) will help constrain the PDFs which will be useful for experiments conducted at the CERN Large Hadron Collider (LHC) in an energy regime where the PDFs are currently not well measured [3].

II. ANALYSIS

This measurement uses an integrated luminosity of approximately 0.7 fb^{-1} of data collected with the D0 detector [4] at the Femilab Tevatron in $p\overline{p}$ collisions at $\sqrt{s} = 1.96$ TeV during 2004-2005. Outgoing partons created in the scattering hadronize to produce jets of particles which are detected in the finely segmented liquid-argon and uranium

calorimeter, which covers most of the solid angle. The central calorimeter (CC) covers the pseudorapidity region $|\eta| < 1.1$, ($\eta = -\ln[\tan(\theta/2)]$ where θ is the angle with respect to the proton beam direction), and the two end cap calorimeters (EC) extend the coverage up to $|\eta| < 4.2$. The intercryostat region (ICR) between the CC and EC contains scintillator-based detectors that supplement the coverage of the calorimeter. Massive jets are reconstructed by clustering energy deposited in the calorimeter towers using the Run II iterative seed-based cone jet algorithm including midpoints with cone radius $\mathcal{R} = \sqrt{(\Delta\phi)^2 + (\Delta y)^2} = 0.7$, where ϕ is the azimuthal angle [5]. The measurement is made in six different rapidity regions: $0 < |y|_{\max} < 0.4$ (CC1), $0.4 < |y|_{\max} < 0.8$ (CC2), $0.8 < |y|_{\max} < 1.2$ (ICR1), $1.2 < |y|_{\max} < 1.6$ (ICR2), $1.6 < |y|_{\max} < 2,0$ (EC1), and $2.0 < |y|_{\max} < 2.4$ (EC2), where $|y|_{\max}$ is the rapidity of the jet with the largest $|y|$ of the two leading jets ordered in p_T.

Events are required to satisfy jet trigger requirements with minimum dijet mass thresholds in a region. Triggers efficiencies are studied by comparing triggers with higher thresholds to triggers with lower thresholds in regions where the latter trigger is 100% efficient. The trigger with the lowest threshold was determined to be 100% efficient by comparing with an independent sample of muon triggered events. In the CC and ICR, single jet triggers are measured to be efficient and have well behaved turn on properties, while dijet triggers with a minimum dijet mass ($M_{\rm JJ}$) threshold have these preferred properties in the EC and are used. Triggers are used in the analysis only in regions where they are greater than 99% efficient.

Events are required to pass data quality cuts and jet quality cuts. Jets are generally required to have less than 5% of their energy deposited in the electromagnetic section of the calorimeter. The two highest p_T jets must have $p_T > 40$ GeV.

The measured value of the energy of each jet is not the same as the energy of the jet made of the stable particles entering the calorimeter due to the energy response of the calorimeter, energy showering in and out the jet cone, and additional energy from event pileup and multiple proton interactions. A jet energy scale (JES) correction for these effects is determined using the p_T imbalance in γ + jet events in the region where $|\eta| < 0.4$, and using events with only two jets when one jet has $|\eta| < 0.4$ and other jet has any η. Additionally, since the dijet sample is dominated by gluon initiated jets, corrections of a few percent due to the difference in response between quark and gluon initiated jets are computed using the PYTHIA event generator [6], and passed through a GEANT based simulation of the detector response [7]. Once all of these corrections are applied, typically on the order of 50% for a jet energy of 50 GeV, and 20% for a jet energy of 400 GeV, the jet four momentum is determined at the particle level excluding muon and neutrino energies, except for resolution and inefficiency effects. This corrected value is used to determine the dijet mass.

The position of the $p\overline{p}$ interaction is reconstructed using a tracking system consisting of silicon microstrip detectors and scintillating fibers located inside a solenoidal magnetic field of approximately 2 T. The position of this primary vertex along the beam line is required to be within 50 cm of the detector center. This requirement is 93.0±0.5% efficient for signal events. In order to suppress cosmic ray events, $\not\!\!E_T/P_T^{\rm max} < 0.7$ where $\not\!\!E_T$ is the transverse component of the vector sum of the momenta in calorimeter cells and $p_T^{\rm max}$ is the transverse momentum of the jet with the maximum p_T. Requirements on characteristics of shower shape development are used to remove the remaining background due to electrons, photons, and detector noise that mimic jets. The efficiency for these requirements is $> 99\%$ ($> 97.5\%$ in the ICR). After all these requirements, the background is $< 0.1\%$ in our sample.

Because the underlying dijet mass spectrum is steeply falling, the measured spectrum is systematically shifted to higher mass values due primarilly to jet energy resolution. The jet p_T resolution is measured using the p_T imbalance in events with only two jets, and is found to be about 13% at $p_T \sim 50$ GeV decreasing to about 7% at $p_T \sim 400$ GeV in the CC and EC, and to be about 16% at $p_T \sim 50$ GeV decreasing to about 11% at $p_T \sim 400$ GeV in the ICR. The data is corrected to the "particle level" as defined in Ref. [8]. These corrections for migrations between bins and for other experimental effects are determined using a parameterized model of the detector with resolutions obtained from the data. This detector model uses events generated by PYTHIA (Tune QW, MSTW2008LO PDFs) [9] that have been reweighted to match measured distributions in the data. The model is then used to correct the dijet mass cross section for various detector effects, including η and ϕ resolutions, misvertexing where the wrong primary vertex was used, jet identification (ID) efficiency, rapidity bias, and the missing muon and neutrino energies removed by the jet energy correction. The total experimental corrections vary from 3% at $M_{JJ} \sim 400$ GeV to 12% at 1000 GeV in the CC, from 0.5% at $M_{JJ} \sim 400$ GeV to 2% at 1000 GeV in the ICR, and from 1% at $M_{JJ} \sim 500$ GeV to 6% at 1000 GeV in the EC. Bin size in $M_{\rm JJ}$ are chosen to be about twice the mass resolution and to have an efficiency and purity of about 50% as determined using the parameterized detector model, where efficiency is defined as the ratio of Monte Carlo events reconstruceted to those generated in a certain M_{JJ} bin and purity is defined as the ratio of Monte Carlo events generated and reconstructed in a certain M_{JJ} bin to all events in that bin.

III. RESULTS

The fully corrected dijet mass spectrum is calculated using Eq. 1

$$d^2\sigma/dM_{\rm JJ}\, d|y|_{\rm max} = (N_{\rm evt}C)/(\mathcal{L}\,\epsilon_{\rm vtx}\,\Delta M_{\rm JJ}\,\Delta|y|_{\rm max}) \quad (1)$$

where $N_{\rm evt}$ is the number of events, $\mathcal{L}$ is the luminosity, $\epsilon_{\rm vtx}$ is the vertex efficiency, $\Delta M_{\rm JJ}$ is the mass bin width, $\Delta|y|_{\rm max}$ is the rapidity bin width, and C is the correction factor for detector effects as described above. The dijet mass spectra in all six rapidity regions are plotted in Fig. 1. The data are compared to the next-to-leading order (NLO) prediction computed using fastNLO [10] based on NLO++[11, 12] for MSTW2008NLO PDFs [13] and the corresponding value of $\alpha_s(M_Z) = 0.120$." The NLO prediction was corrected for hadronization and underlying event effects using correction factors which range between 5% and 20% in all rapidity region and were obtained by turning these effects on and off individually in PYTHIA. The renormalization and factorization scales are set to $\mu_R = \mu_F = p_T = (p_{T1} + p_{T2})/2$ where p_{T1} and p_{T2} are the transverse momentum of the two jets used to form the dijet mass. The effect of varying these scales from $\mu = p_T/2$ to $\mu = 2p_T$ is shown. The ratio of data to theory is shown in Fig. 2.

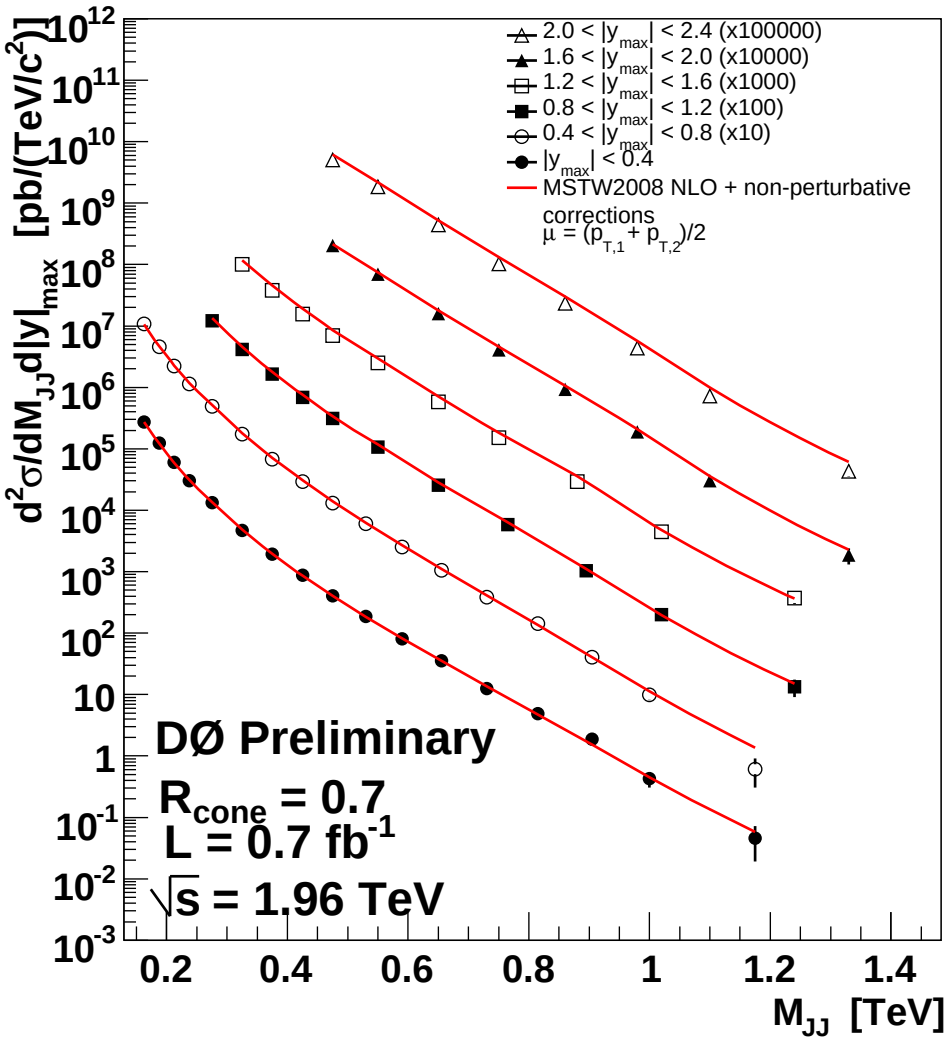

FIG. 1: The dijet mass spectrum for fully corrected data. Uncertainties shown are statistical only.

The systematic uncertainties in this analysis are dominated by the uncertainties in the jet energy scale (JES), which range from 10% to 20% in the CC, 15% to 30% in the ICR and 20% to 40% in the EC region. The second largest

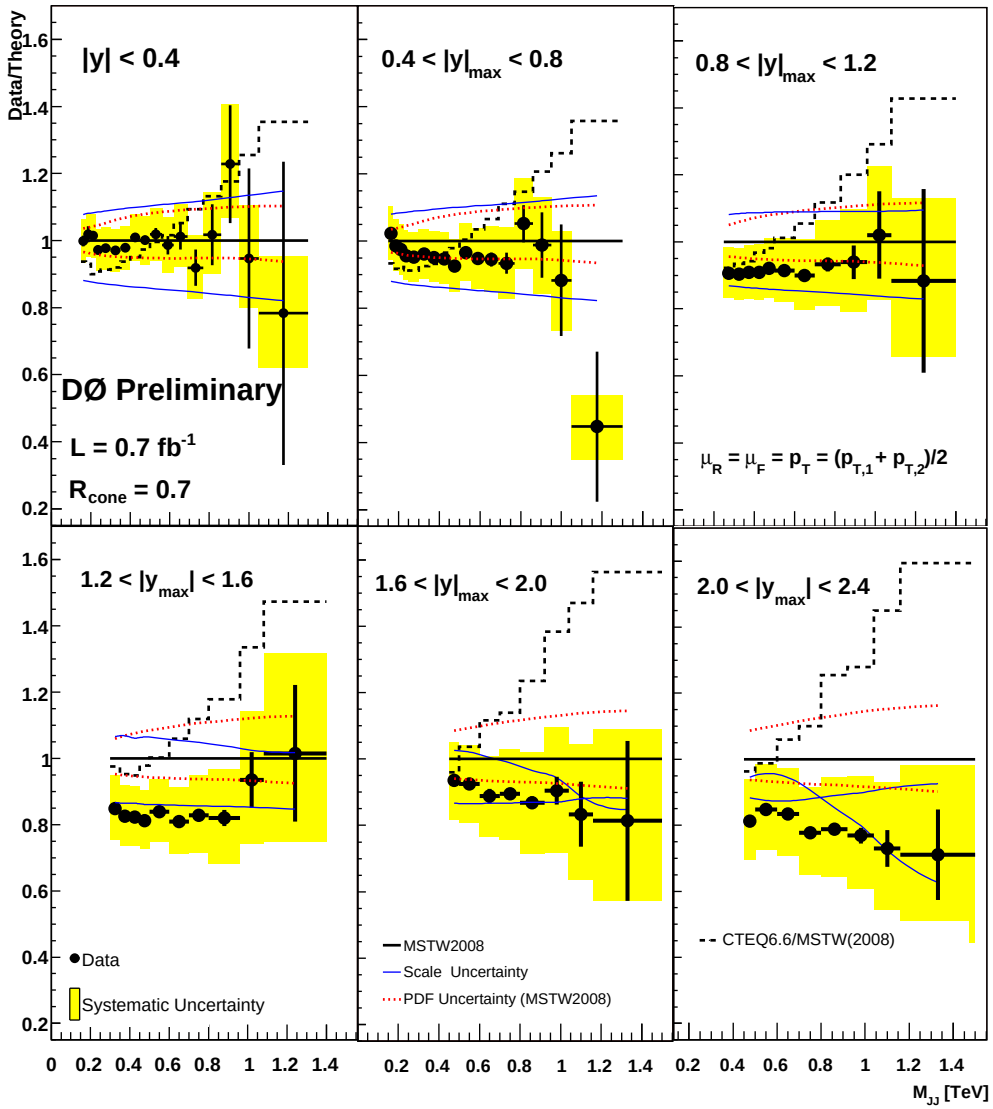

FIG. 2: Data over theory ratio in all 6 $|y|_{\max}$ bins. The systematic uncertainty from data is shown as a yellow band. There is an additional completely correlated uncertainty of 6% due to luminosity not shown in the plots. The legend for all six plots is shown spread out over the 3 bottom plots.

systematic uncertainty comes from the p_T resolution uncertainty, which ranges between 2% and 10% in all regions. The luminosity has an uncertainty of 6% which is completely correlated across all dijet mass bins. Certain systematic uncertainties are calculated using the parameterized model of the detector including jet ID efficiency corrections, corrections due to misvertexing and the angular resolutions, and an uncertainty due to the Monte Carlo reweighting. These are all small, on the order of less than 2% in all regions.

The systematic uncertainties are similar in size to both the PDF and scale uncertainties, suggesting that the measurement will constrain future theoretical predictions. We are quoting PDF uncertainties corresponding to a 90% confidence level [13]. These uncertainties are smaller than earlier measurements at this energy [2]. In addition to comparing to the MSTW PDFs [13], we also present theoretical predictions using CTEQ6.6 [14]. We see that the difference in the cross section due to different PDFs can be 40-60% at the highest mass. The MSTW PDFs are clearly favored. However one should note that the MSTW PDFs include Tevatron Run II jet data and exclude Run I jet data, while CTEQ6.6 does not include Run II jet data. This precise measurement of the dijet mass cross section will be used to constrain models of new physics.

We thank the staffs at Fermilab and collaborating institutions, and acknowledge support from the DOE and

NSF (USA); CEA and CNRS/IN2P3 (France); FASI, Rosatom and RFBR (Russia); CNPq, FAPERJ, FAPESP and FUNDUNESP (Brazil); DAE and DST (India); Colciencias (Colombia); CONACyT (Mexico); KRF and KOSEF (Korea); CONICET and UBACyT (Argentina); FOM (The Netherlands); STFC (United Kingdom); MSMT and GACR (Czech Republic); CRC Program, CFI, NSERC and WestGrid Project (Canada); BMBF and DFG (Germany); SFI (Ireland); The Swedish Research Council (Sweden); CAS and CNSF (China); and the Alexander von Humboldt Foundation (Germany).

[1] E. Eichten, K. Lane, and M.E. Peskin, Phys. Rev. Lett. **50**, 811 (1983); E. Eichten, I. Hinchcliffe, K. Lane, and C. Quigg, Rev. Mod.Phys. **56**, 579 (1984), Addendum *ibid.* **58**, 1065 (1986); K. Lane, arXiv:hep-ph/9605257, (1996).
[2] T. Aaltonen *et al* (CDF Collaboration), "Search for new particles decaying into dijets in proton-antiproton collisions at $\sqrt{s} = 1.96$ TeV", arXiv:0812.4036, [hep-ex] (2008), submitted to Phys. Rev.D.
[3] A. Belyaev *et al.*, J. High Energy Phys. 01 (2006) 069.
[4] V.M. Abazov *et al.* (D0 Collaboration), "The upgraded DØ detector," Nucl. Instrum. Methods Phys. Res. A **565**, 463 (2006).
[5] G.C. Blazey *et al.*, in *Proceedings of the Workshop: QCD and Weak Boson Physics in Run II,* edited by U. Baur, R.K. Ellis, and D. Zeppenfeld, Fermilab-Pub-00/297 (2000).
[6] T. Sjostrand *et al.*, Comput. Phys. Commun. **135**, 238 (2001).
[7] R. Brun and F. Carminati, CERN Program Library Long Writeup Report No. W5013, 1993 (unpublished).
[8] C. Buttar *et al.*, arXiv:0803.0678 [hep-ph], section 9.
[9] M. G. Albrow *et al.* [TeV4LHC QCD Working Group], arXiv:hep-ph/0610012.
[10] T. Kluge, K. Rabbertz, and M. Wobisch, arXiv:hep-ph/0609285.
[11] Z. Nagy, Phys. Rev. D **68**, 094002 (2003).
[12] Z. Nagy, Phys. Rev. Lett. **88**, 122003 (2002).
[13] A.D. Martin, W.J. Stirling, R.S Thorne, G. Watt, arXiv:0901.0002v2, [hep-ph] (2009), submitted to Eur. Phys. Jour. C.
[14] P.M. Nadolsky *et.al.*, "Implications of CTEQ global analysis for collider observables," Phys Rev, D, 78:013004 (2008).